

# Kinetic effects of temperature on rates of genetic divergence and speciation

Andrew P. Allen<sup>\*†</sup>, James F. Gillooly<sup>‡</sup>, Van M. Savage<sup>§</sup>, and James H. Brown<sup>†¶</sup>

<sup>\*</sup>National Center for Ecological Analysis and Synthesis, 735 State Street, Suite 300, Santa Barbara, CA 93101; <sup>‡</sup>Department of Zoology, University of Florida, Gainesville, FL 32611; <sup>§</sup>Bauer Center for Genomics Research, Harvard University, Boston, MA 02138; and <sup>¶</sup>Department of Biology, University of New Mexico, Albuquerque, NM 87131

Contributed by James H. Brown, May 2, 2006

Latitudinal gradients of biodiversity and macroevolutionary dynamics are prominent yet poorly understood. We derive a model that quantifies the role of kinetic energy in generating biodiversity. The model predicts that rates of genetic divergence and speciation are both governed by metabolic rate and therefore show the same exponential temperature dependence (activation energy of  $\approx 0.65$  eV;  $1 \text{ eV} = 1.602 \times 10^{-19} \text{ J}$ ). Predictions are supported by global datasets from planktonic foraminifera for rates of DNA evolution and speciation spanning 30 million years. As predicted by the model, rates of speciation increase toward the tropics even after controlling for the greater ocean coverage at tropical latitudes. Our model and results indicate that individual metabolic rate is a primary determinant of evolutionary rates:  $\approx 10^{13} \text{ J}$  of energy flux per gram of tissue generates one substitution per nucleotide in the nuclear genome, and  $\approx 10^{23} \text{ J}$  of energy flux per population generates a new species of foraminifera.

allopatric speciation | biodiversity | macroevolution | metabolic theory of ecology | molecular clock

The latitudinal increase in biodiversity from the poles to the equator is the most pervasive feature of biogeography. For two centuries, since the time of von Humboldt, Darwin, and Wallace, scientists have proposed hypotheses to explain this pattern. New species arise through the evolution of genetic differences among populations from a common ancestral lineage (1–4). Many hypotheses therefore attribute the latitudinal biodiversity gradient to a gradient in speciation rates caused by some independent variable, such as earth surface area or solar energy input (5–7). Some fossil data suggest that speciation rates do indeed increase toward the tropics (8–10), but these findings remain open to debate due in part to our limited understanding of the factors that control macroevolutionary dynamics.

Recent advances toward a metabolic theory of ecology (11) provide new opportunities for assessing the factors that control speciation rates. This recent work indicates that two fundamental variables influencing the tempo of evolution, the generation time, and the mutation rate (3) are both direct consequences of biological metabolism (12–14). Here we combine these recent insights from metabolic theory with the theory of population genetics to derive a model that predicts how environmental temperature, through its effects on individual metabolic rates (Eqs. 1–4), influences rates of genetic divergence among populations (Eqs. 5–7) and rates of speciation in communities (Eqs. 8 and 9). We evaluate the model by using data from planktonic foraminifera, because this group has extensive DNA sequence data for evaluating population-level predictions on genetic divergence combined with an exceptionally complete fossil record for evaluating community-level predictions on speciation rates.

## Model Development

The two individual-level variables constraining the evolutionary rate of a population, the generation time, and the mutation rate (3) are both direct consequences of biological metabolism (15, 16). They are both governed by the body size- and temperature-

dependence of mass-specific metabolic rate,  $\bar{B}$  ( $\text{J} \cdot \text{sec}^{-1} \cdot \text{g}^{-1}$ ) (12–14):

$$\bar{B} = B/M = b_o M^{-1/4} e^{-E/kT} = B_o e^{-E/kT}, \quad [1]$$

where  $B$  is individual metabolic rate ( $\text{J} \cdot \text{sec}^{-1}$ ),  $M$  is body mass ( $\text{g}$ ),  $T$  is absolute temperature ( $\text{K}$ ),  $B_o$  is a normalization parameter independent of temperature ( $\text{J} \cdot \text{sec}^{-1} \cdot \text{g}^{-1}$ ) that varies with body size as  $B_o = b_o M^{-1/4}$  (12), and  $b_o$  is a normalization parameter independent of body size and temperature that varies among taxonomic and functional groups (12, 17). The Boltzmann–Arrhenius factor,  $e^{-E/kT}$ , characterizes the exponential effect of temperature on metabolic rate, where  $E$  is the average activation energy of the respiratory complex ( $\approx 0.65$  eV;  $1 \text{ eV} = 1.602 \times 10^{-19} \text{ J}$ ), and  $k$  is the Boltzmann constant ( $8.62 \times 10^{-5} \text{ eV} \cdot \text{K}^{-1}$ ). This Boltzmann–Arrhenius factor has been shown to describe the temperature dependence of metabolic rate for a broad assortment of organisms in recent work (12) and in much earlier work conducted near the beginning of the last century (18).

Recent work indicates that the generation time, expressed here as the individual turnover rate,  $g$  (generations  $\text{sec}^{-1}$ ), and the mutation rate,  $\alpha$  (mutations  $\cdot \text{nucleotide}^{-1} \cdot \text{sec}^{-1}$ ), both show this same temperature dependence (12–14):

$$g = g_o \bar{B} = g_o B_o e^{-E/kT} \quad [2]$$

and

$$\alpha = \alpha_o \bar{B} = \alpha_o B_o e^{-E/kT}, \quad [3]$$

where  $g_o$  is the number of generations per joule of energy flux through a gram of tissue (generations  $\cdot \text{J}^{-1} \cdot \text{g}$ ), and  $\alpha_o$  is the number of mutations per nucleotide per joule of energy flux through a gram of tissue (mutations  $\cdot \text{nucleotide}^{-1} \cdot \text{J}^{-1} \cdot \text{g}$ ). Eqs. 2 and 3 predict a 15-fold increase in the rates of individual turnover and mutation over the temperature range  $0$ – $30^\circ\text{C}$  from the poles to the equator ( $e^{-E/k303}/e^{-E/k273} = 15$ -fold from  $273$ – $303 \text{ K}$ ). Because  $g$  and  $\alpha$  are both governed by  $\bar{B}$ , the number of mutations per nucleotide per generation,

$$\alpha_\tau = \alpha/g = \alpha_o/g_o \propto e^{0/kT}, \quad [4]$$

is independent of temperature.

Speciation entails genetic divergence among populations from a common ancestral lineage, resulting in reproductive isolation (2, 4). The theory of population genetics characterizes the rate of increase in the total genetic divergence,  $D$  (substitutions  $\text{nucleotide}^{-1}$ ), between two reproductively isolated diploid pop-

Conflict of interest statement: No conflicts declared.

Freely available online through the PNAS open access option.

Abbreviations: CI, confidence interval; FO, first occurrence; Ma, mega-annum; SSU rDNA, small subunit rDNA-encoding DNA.

<sup>†</sup>To whom correspondence may be addressed. E-mail: drewa@nceas.ucsb.edu or jhbrown@unm.edu.

© 2006 by The National Academy of Sciences of the USA



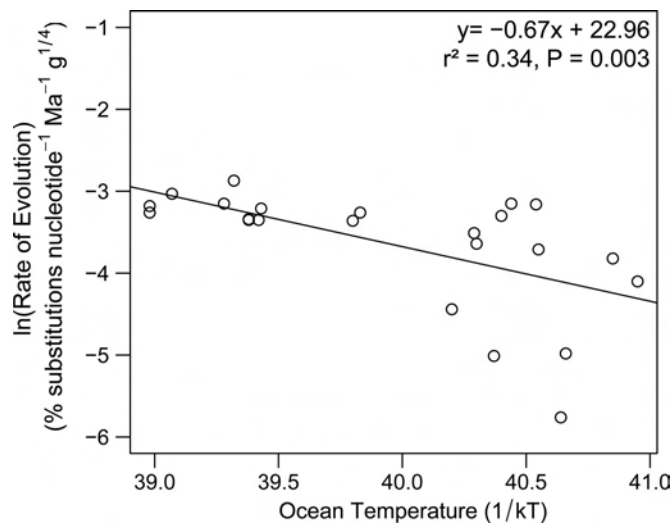


**Fig. 1.** Effect of ocean temperature,  $1/kT$ , on the size-corrected rate of neutral molecular evolution,  $\ln(f_0\alpha M^{1/4})$ , for nuclear genomes of planktonic foraminifera. The slope ( $-0.67$  eV) was fitted by using ordinary least-squares regression and is close to the value of  $-E \approx -0.65$  eV (95% CI,  $-0.26$  to  $-1.07$  eV), which was predicted based on the temperature dependence of individual metabolic rate (Eq. 3). Refer to Appendix 1 for details on this global compilation of SSU rDNA data.

temperature-dependence of nuclear DNA evolution matches the prediction derived in Eq. 3 based on the activation energy of individual metabolic rate. Importantly, we derive this relationship by characterizing habitat temperatures by using sea-surface temperature data for shallow-dwelling taxa and temperatures at 200-m depth for deeper-dwelling taxa (see Appendix 1). If, instead, we characterize habitat temperatures by using sea-surface temperature data for all taxa, the slope of the relationship between  $\ln(f_0\alpha M^{1/4})$  and  $1/kT$  still yields a 95% CI for  $E$  that includes the predicted value of 0.65 eV (0.04–1.45 eV), but the correlation is weaker ( $r^2 = 0.18$  versus 0.34 for the model in Fig. 1). This finding supports the hypothesis that deeper-dwelling taxa exhibit lower size-corrected rates of molecular evolution as a direct consequence of declines in habitat temperature with increasing depth. Thus, it appears that thermal habitat preference significantly influences rates of DNA evolution for this group.

The results in Fig. 1 represent previously unrecognized and direct evidence, based on well established fossil calibrations (see Appendix 1), that absolute rates of DNA evolution increase exponentially with environmental temperature in the same way as individual metabolic rate. These results also serve to reinforce and extend previous work indicating that absolute rates of mitochondrial DNA evolution are higher for warmer-bodied endotherms than for ectothermic animals of similar size (14, 16) and that relative rates of nuclear DNA evolution increase with environmental temperature for plants (27–29). Note that our model predicts that rates of molecular evolution should increase exponentially with environmental temperature for ectotherms but not for endotherms, which maintain body temperatures of  $\approx 35$ – $40^\circ\text{C}$  during active periods, regardless of ambient temperature. Hence, our model and results do not contradict a study of birds, which found “no support for an effect of latitude on rate of molecular evolution” (30).

We evaluate the predicted temperature dependence for the genetic divergence between incipient species,  $D_s$ , in Eq. 7, by using a global compilation of SSU rDNA data for  $>20$  “cryptic” taxa (23) that have been identified within seven morphospecies of planktonic foraminifera (see Appendix 2, which is published

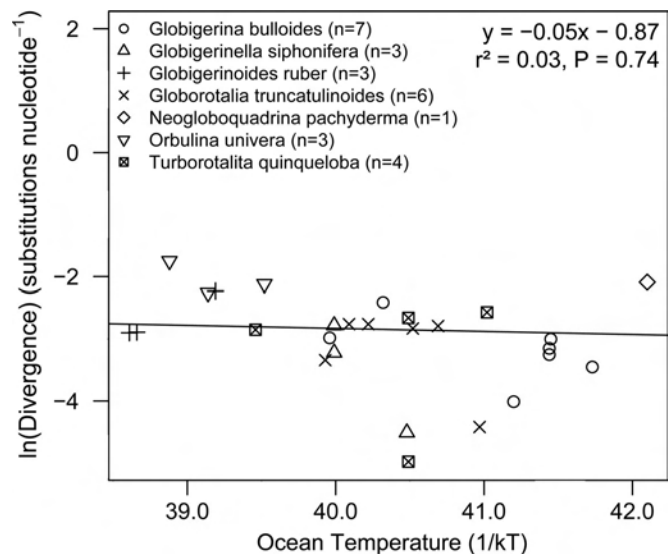


**Fig. 2.** Effect of ocean temperature,  $1/kT$ , on genetic divergence,  $\ln(D_s)$ , for nuclear genomes of ecologically distinct genotypes within seven morphospecies of planktonic foraminifera. The sample sizes in the legend refer to the numbers of pairwise comparisons among populations comprising each morphospecies. The data were weighted such that each morphospecies contributed equally to the ordinary least-squares regression slope, which does not differ from the predicted value of 0 (Eq. 7). This conclusion remains unchanged if data points, rather than morphospecies, are weighted equally ( $P = 0.10$ ). Refer to Appendix 2 for details on this global compilation of SSU rDNA data.

as supporting information on the PNAS web site). These cryptic taxa are ecologically distinct genotypes with different geographic distributions (21–24, 31) and temperature optima (23). They are therefore thought to represent incipient morphotaxa in the relatively early stages of speciation (24).

Despite evidence indicating that rates of molecular evolution increase exponentially with environmental temperature (Fig. 1), the genetic divergence between incipient taxa is independent of ocean temperature (Fig. 2;  $P = 0.74$ ), as predicted by Eq. 7. These findings are consistent with Assumptions 1 and 2 of our model that  $D_s^+$ ,  $J_s$ , and  $s$  are all independent of temperature. We note, however, that the data depicted in Fig. 2 encompass taxon pairs at various stages of divergence, not just the incipient stage, which is fleeting and therefore difficult to observe (4).

We evaluate latitudinal gradients in rates of speciation at the level of metacommunities,  $V_m$  (Eq. 9), by using fossil data compiled in the Neptune database, which span the last 30 million years (Ma) of macroevolution for planktonic foraminifera (32). Our analysis involves assessing how the rate of first occurrence (FO) of new morphospecies, which is a surrogate measure for the speciation rate (10), varies across latitudes at the global scale. When analyzing and interpreting these data, it is important to recognize that each morphospecies may evolve to comprise several distinct genotypes that occupy different thermal environments, as shown in Fig. 2.

By using these fossil data, we show that the time-averaged rate of speciation is significantly higher in the tropics (Fig. 3A, equal-area latitudinal bands 2 and 3) than in the temperate zones (Fig. 3A, bands 1 and 4), even after controlling for sampling effort and for the greater habitat area at tropical latitudes (Fig. 3B; and see Appendix 3, which is published as supporting information on the PNAS web site). Furthermore, this gradient in macroevolutionary dynamics is significantly correlated with average ocean temperatures ( $r^2 = 0.97$ ;  $P = 0.01$ ; Fig. 3B), which have been estimated by using a robust paleotemperature calibration (33) to control for the  $\approx 8^\circ\text{C}$  decline in high-latitude ocean temperatures





population-level processes to determine the temperature-dependence of speciation rates (Eq. 8).

The fourth insight is that habitat area is also an important determinant of latitudinal gradients in speciation rates and hence biodiversity, as suggested by Rosenzweig (6). In fact, our model and results indicate that the predicted exponential effects of temperature on speciation rates are only manifested after controlling for habitat area and community abundance by expressing speciation on a per capita basis (Eq. 8). This approach runs counter to the long-standing tradition among evolutionary biologists and paleontologists of expressing speciation on a per species basis (species·species<sup>-1</sup>·time<sup>-1</sup>) (4). Nevertheless, it is consistent with evolutionary theory, because speciation occurs at the level of populations (Eqs. 5–9). It is also consistent with the recently proposed neutral biodiversity theory (NBT) of Hubbell (26), which predicts that the per capita speciation rate,  $\nu$ , determines the number of species maintained in a metacommunity of fixed abundance  $J_m$ . Synthesizing our energetically and genetically based model of speciation (Eqs. 1–9) with NBT may therefore yield a better understanding of why biodiversity increases exponentially with environmental temperature in the same way as individual metabolic rate for diverse groups of terrestrial, aquatic, and marine ectotherms (7, 40, 41).

We conclude by noting that the theory developed here also predicts that evolutionary rates vary as a power function with body size according to the mass-dependence of individual metabolic rate ( $\propto M^{-1/4}$ ). This result has been shown for rates of microevolution, i.e., nucleotide substitution (14), but has not yet been demonstrated for rates of macroevolution. Extension of our model may therefore yield insights into the combined effects of body size and temperature on other prominent yet poorly understood gradients in macroevolutionary dynamics (for examples, see refs. 42 and 43).

## Methods

**Molecular Evolution Data.** The SSU rDNA data in Fig. 1 were compiled from the sources cited in Appendix 1. Our model predicts that rates of molecular evolution increase exponentially with temperature (Eq. 3), which implies that the warmer, more rapidly evolving taxon makes a greater contribution to the genetic divergence,  $D$ , and hence to the calculated rate of molecular evolution  $f_o\alpha = D/2\Gamma$  (following Eq. 5), where  $\Gamma$  is the time since divergence. To account for the greater contribution of the warmer-bodied taxon to  $f_o\alpha$ , we characterize the overall habitat temperature for each taxon pair depicted in Fig. 1 by using the Boltzmann average,

$$\langle T \rangle_E = -E / \ln((e^{-E/kT_1} + e^{-E/kT_2})/2)k,$$

where  $T_1$  and  $T_2$  are the habitat temperatures of the two taxa in Kelvins. Habitat temperatures were independently estimated by using a global compilation of contemporary community abundance data collected from 1,265 sites around the world (44) in conjunction with contemporary ocean temperature data (45). Habitat temperatures were estimated by using sea-surface temperatures for shallow-dwelling taxa and temperatures at 200-m depth for deeper-dwelling taxa (Appendix 1).

**Genetic Divergence Data.** The SSU rDNA data in Fig. 2 were compiled from the sources cited in Appendix 2. The habitat temperature of each population was estimated from the spatial location of sampling by using contemporary ocean temperature data (45). The Boltzmann-averaged habitat temperature,  $\langle T \rangle_E$ , was then calculated for each taxon pair depicted in the figure.

**FO Data.** The latitudinal distribution of FOs of morphospecies in Fig. 3B was analyzed by using morphospecies-level data in the Neptune database, a compilation of fossil samples from over 160 deep-sea drilling holes around the world that have been dated to an average precision of <1 Ma (32). We analyzed the Neptune data by using the following procedure to simultaneously control for latitudinal variation in area (Fig. 3A) and for the effects of sampling effort on paleontological analyses (46): (i) We assigned each of >3,000 core samples to one of four latitudinal bands of equal ocean surface area (Fig. 3A) and to one of six 5-Ma time intervals spanning the last 30 Ma. (ii) We selected a subset of 40 samples at random and without replacement from each equal-area latitudinal band and time interval, yielding a data subset comprising >900 samples. (iii) We determined the band of FO for each morphospecies of foraminifera arising through speciation over the past 30 Ma. (iv) We tallied the total number of FOs in each band to obtain estimates for  $V_m$ . (v) We repeated steps ii–iv 100 times to generate the 95% CIs for  $V_m$  depicted in Fig. 3B (Appendix 3).

**Paleotemperature Data.** To obtain the estimates of average ocean temperature depicted in Fig. 3B,  $1/kT$ , we modeled variation in sea-surface temperatures with respect to latitude,  $L$  ( $-90^\circ$  to  $90^\circ$ N), and time,  $t$ , by using the heat equation on the surface of a sphere,  $T(L, t) = (P(t) - T_0)\sin^2(\pi L/180) + T_0$ , where  $P(t)$  is the sea-surface temperature at the poles at time  $t$ , and  $T_0$  is the sea-surface temperature at the equator. The function  $P(t)$  was estimated in Fig. 2 of ref. 33 by using robust methods of paleotemperature calibration. The parameter  $T_0$  was assumed to remain constant at  $\approx 28^\circ\text{C}$  over the past 30 Ma based on available evidence (47). The function  $T(L, t)$  was integrated over time and space, as described in Appendix 4, to yield the estimates of  $1/kT$  depicted in Fig. 3B.

**Estimating the per Capita Speciation Rate.** Evaluating the temperature dependence of the per capita speciation rate (Eq. 8) required explicitly accounting for temperature-dependent changes in foraminifera community abundance across latitudes. To avoid difficulties associated with inferring live abundances of foraminifera from shell accumulation rates, we characterized this temperature dependence by using a global compilation of plankton tow data (45) on foraminifer metacommunity abundance per unit area,  $J_A$ . We estimated the temperature dependence of the per capita speciation rate, characterized by  $E$  (Eq. 8), and the normalization parameter,  $\nu_o$ , by expressing the latitudinal distribution of FOs as a cumulative function of ocean area (Fig. 3A), paleotemperature  $T(L, t)$ , and metacommunity abundance (Appendix 5).

**Estimating the Energy Required to Induce Mutations.** Following Eqs. 2–5, the size- and temperature-corrected rate of molecular evolution,  $f_o\alpha M^{1/4}e^{E/kT}$ , is equal to  $f_o\alpha b_o$ . For primates, we obtain an estimate of  $2.5 \times 10^{13} \text{ J} \cdot \text{g}^{-1} \cdot \text{substitutions}^{-1} \cdot \text{nucleotide}$  for  $1/f_o\alpha b_o$  by using an estimate of  $b_o \approx 3.9 \times 10^8 \text{ W} \cdot \text{g}^{-3/4}$  for endotherms (17) and the geometric mean of the estimates of  $f_o\alpha M^{1/4}e^{E/kT}$  in ref. 14 for the globin gene ( $\approx 4.9 \times 10^{10} \text{ substitutions} \cdot \text{nucleotide}^{-1} \cdot 10^{-8} \text{ yr} \cdot \text{g}^{1/4}$ ). For planktonic foraminifera, we obtain an estimate of  $1.8 \times 10^{13} \text{ J} \cdot \text{g}^{-1} \cdot \text{substitutions}^{-1} \cdot \text{nucleotide}$  for  $1/f_o\alpha b_o$  by using an estimate of  $b_o \approx 2.8 \times 10^7 \text{ W} \cdot \text{g}^{-3/4}$  for unicells (17) and the geometric mean of the estimates of  $f_o\alpha M^{1/4}e^{E/kT}$  for the data depicted in Fig. 1 ( $\approx 5.0 \times 10^9 \text{ substitutions} \cdot \text{nucleotide}^{-1} \cdot 10^{-8} \text{ yr} \cdot \text{g}^{1/4}$ ).

We thank Fangliang He, Andrew Martin, Richard Norris, Klaus Rohde, and John Wilkins for their insightful comments and suggestions. A.P.A. was supported as a Postdoctoral Associate at the National Center for Ecological Analysis and Synthesis, a center funded by National Science Foundation Grant DEB-0072909, and the University of California, Santa Barbara. V.M.S. was supported by National Institutes of Health Grant 1 P50 GM68763-02 through the Bauer Center for Genomics Research.



## Appendix 1

Global compilation of SSU rDNA data depicted in Fig. 1, along with citations of data sources and descriptions of variables. The designations (S) and (D) for the species pairs below refer to shallow- and deeper-dwelling taxa.

|  | I. Body Size (g) |          |                       | II. Temperature (°C) |       |                       |  | III. Div. Time (Ma) |                |             | IV. Divergence |              | V. Rate                  |        |                           |
|--|------------------|----------|-----------------------|----------------------|-------|-----------------------|--|---------------------|----------------|-------------|----------------|--------------|--------------------------|--------|---------------------------|
| Species pair   | $M_1$            | $M_2$    | $\langle M \rangle_q$ | $T_1$                | $T_2$ | $\langle T \rangle_E$ |  | $\Gamma_{min}$      | $\Gamma_{max}$ | Source<br>s | $D$            | Sources      | $f_s \alpha = D/2\Gamma$ | $1/kT$ | $\ln(f_s \alpha M^{1/4})$ |
| <i>Globigerina bulloides</i> (D) / <i>Globigerina falconensis</i> (S)          | 1.96E-05         | 7.80E-06 | 1.20E-05              | 9                    | 18    | 14                    |  | 18                  | 18.6           | (1)         | 0.229          | (2)          | 0.626                    | 40.40  | -3.30                     |
| <i>Globigerinella siphonifera</i> (D) / <i>Globigerina bulloides</i> (D)       | 9.67E-05         | 1.96E-05 | 4.02E-05              | 19                   | 9     | 15                    |  | 27.0                | 29.0           | (3)         | 0.185          | (3)          | 0.330                    | 40.30  | -3.64                     |
| <i>Globigerinella siphonifera</i> (D) / <i>Globigerinella calida</i> (D)       | 9.67E-05         | 5.56E-05 | 7.26E-05              | 19                   | 18    | 18                    |  | 5.0                 | 5.0            | (3)         | 0.038          | (3, 4)       | 0.375                    | 39.80  | -3.36                     |
| <i>Globigerinella siphonifera</i> (D) / <i>Globigerinoides conglobatus</i> (S) | 9.67E-05         | 5.56E-05 | 7.27E-05              | 19                   | 24    | 22                    |  | 25.0                | 25.0           | (5)         | 0.190          | (6)          | 0.381                    | 39.38  | -3.35                     |
| <i>Globigerinella siphonifera</i> (D) / <i>Globigerinoides ruber</i> (S)       | 9.67E-05         | 2.73E-05 | 4.89E-05              | 19                   | 24    | 22                    |  | 25.0                | 25.0           | (5)         | 0.213          | (6)          | 0.425                    | 39.38  | -3.34                     |
| <i>Globigerinella siphonifera</i> (D) / <i>Globigerinoides sacculifer</i> (S)  | 9.67E-05         | 9.58E-05 | 9.63E-05              | 19                   | 25    | 22                    |  | 25.0                | 28.5           | (3, 5)      | 0.231          | (6)          | 0.431                    | 39.28  | -3.15                     |
| <i>Globigerinoides ruber</i> (S) / <i>Globigerinoides conglobatus</i> (S)      | 2.73E-05         | 5.56E-05 | 3.84E-05              | 24                   | 24    | 24                    |  | 5.0                 | 10.0           | (3)         | 0.092          | (3, 4, 6-9)  | 0.613                    | 39.07  | -3.03                     |
| <i>Globigerinoides ruber</i> (S) / <i>Globigerinoides sacculifer</i> (S)       | 2.73E-05         | 9.58E-05 | 4.87E-05              | 24                   | 25    | 25                    |  | 25.0                | 28.5           | (3)         | 0.245          | (3, 6, 7)    | 0.459                    | 38.98  | -3.26                     |
| <i>Globigerinoides ruber</i> (S) / <i>Orbulina universa</i> (S)                | 2.73E-05         | 3.10E-04 | 7.67E-05              | 24                   | 18    | 21                    |  | 17.0                | 25.0           | (9)         | 0.157          | (7, 9)       | 0.374                    | 39.42  | -3.35                     |
| <i>Globigerinoides sacculifer</i> (S) / <i>Globigerinoides conglobatus</i> (S) | 9.58E-05         | 5.56E-05 | 7.23E-05              | 25                   | 24    | 25                    |  | 25.0                | 28.5           | (3, 5)      | 0.242          | (6, 7)       | 0.452                    | 38.98  | -3.18                     |
| <i>Globigerinoides sacculifer</i> (S) / <i>Orbulina universa</i> (S)           | 9.58E-05         | 3.10E-04 | 1.65E-04              | 25                   | 18    | 22                    |  | 16.4                | 21.7           | (3)         | 0.191          | (3, 4, 6, 7) | 0.501                    | 39.32  | -2.87                     |
| <i>Globorotalia hirsuta</i> (D) / <i>Globorotalia inflata</i> (D)              | 3.86E-05         | 1.91E-05 | 2.67E-05              | 14                   | 10    | 12                    |  | 17.0                | 18.5           | (3)         | 0.034          | (3)          | 0.096                    | 40.66  | -4.98                     |
| <i>Globorotalia menardii</i> (D) / <i>Globorotalia hirsuta</i> (D)             | 1.26E-04         | 3.86E-05 | 6.67E-05              | 16                   | 14    | 15                    |  | 15.8                | 19.0           | (3)         | 0.115          | (3)          | 0.330                    | 40.29  | -3.51                     |
| <i>Globorotalia menardii</i> (D) / <i>Globorotalia inflata</i> (D)             | 1.26E-04         | 1.91E-05 | 4.39E-05              | 16                   | 10    | 13                    |  | 17.0                | 19.0           | (3)         | 0.108          | (3)          | 0.300                    | 40.55  | -3.71                     |
| <i>Globorotalia menardii</i> (D) / <i>Globorotalia truncatulinoides</i> (D)    | 1.26E-04         | 1.27E-04 | 1.26E-04              | 16                   | 12    | 14                    |  | 15.8                | 19.0           | (3)         | 0.140          | (3)          | 0.402                    | 40.44  | -3.15                     |
| <i>Globorotalia truncatulinoides</i> (D) / <i>Globorotalia hirsuta</i> (D)     | 1.27E-04         | 3.86E-05 | 6.69E-05              | 12                   | 14    | 13                    |  | 7.4                 | 10.5           | (3)         | 0.084          | (3, 4)       | 0.469                    | 40.54  | -3.16                     |
| <i>Globorotalia truncatulinoides</i> (D) / <i>Globorotalia inflata</i> (D)     | 1.27E-04         | 1.91E-05 | 4.40E-05              | 12                   | 10    | 11                    |  | 17.0                | 18.5           | (3)         | 0.096          | (3, 4)       | 0.270                    | 40.85  | -3.82                     |
| <i>Neogloboquadrina dutertrei</i> (D) / <i>Globorotalia hirsuta</i> (D)        | 8.14E-05         | 3.86E-05 | 5.51E-05              | 14                   | 14    | 14                    |  | 11.0                | 23.8           | (3)         | 0.027          | (3)          | 0.078                    | 40.37  | -5.01                     |
| <i>Neogloboquadrina dutertrei</i> (D) / <i>Globorotalia inflata</i> (D)        | 8.14E-05         | 1.91E-05 | 3.69E-05              | 14                   | 10    | 12                    |  | 11.0                | 23.8           | (3)         | 0.014          | (3)          | 0.040                    | 40.64  | -5.76                     |

|   |          |          |          |    |    |    |  |      |      |        |       |          |       |       |       |
|---|----------|----------|----------|----|----|----|--|------|------|--------|-------|----------|-------|-------|-------|
| <i>Neogloboquadrina dutertrei</i> (D) / <i>Neogloboquadrina pachyderma</i> (D)  | 8.14E-05 | 5.37E-06 | 1.67E-05 | 14 | 4  | 10 |  | 10.4 | 10.4 | (10)   | 0.054 | (2)      | 0.260 | 40.95 | -4.10 |
| <i>Neogloboquadrina dutertrei</i> (D) / <i>Pulleniatina obliquiloculata</i> (D) | 8.14E-05 | 6.15E-05 | 7.06E-05 | 14 | 17 | 16 |  | 5.8  | 5.8  | (10)   | 0.015 | (11, 12) | 0.129 | 40.20 | -4.44 |
| <i>Orbulina universa</i> (S) / <i>Globigerinella siphonifera</i> (D)            | 3.10E-04 | 9.67E-05 | 1.66E-04 | 18 | 19 | 18 |  | 25.0 | 28.5 | (3, 5) | 0.181 | (6)      | 0.338 | 39.83 | -3.26 |
| <i>Orbulina universa</i> (S) / <i>Globigerinoides conglobatus</i> (S)           | 3.10E-04 | 5.56E-05 | 1.20E-04 | 18 | 24 | 21 |  | 25.0 | 28.5 | (3, 5) | 0.207 | (6, 7)   | 0.387 | 39.43 | -3.21 |

**Body Size.** Foraminifera size is generally reported as maximum shell length,  $l_1$ , but foraminifera shells vary in shape from thin disks (e.g. *Globorotalia menardii*) to nearly perfect spheres (e.g. *Orbulina universa*) (1). To account for these differences in shell shape, we estimated the body mass,  $M_i$  (g), of each morphospecies as  $M_i \approx \rho \left(\frac{4}{3}\right) \pi \left(\frac{l_1}{2}\right) \left(\frac{l_2}{2}\right) \left(\frac{l_3}{2}\right) = \rho \left(\frac{\pi}{6}\right) l_1^3 \left(\frac{l_2}{l_1}\right) \left(\frac{l_3}{l_1}\right)$ , where  $l_2$  and  $l_3$  are the maximum shell widths along the two axes perpendicular to  $l_1$ , assuming that shells are approximately ellipsoidal in shape, and that the density of body tissue is similar to that of water (i.e.,  $\rho \approx 1 \text{ g cm}^{-3}$ ). Estimates of  $l_1$  were obtained from a published compilation (13). Estimates of the relative widths,  $l_2/l_1$  and  $l_3/l_1$ , were obtained by taking measurements of published photographs of specimens (1, 14). The product of the relative dimensions,  $(l_2/l_1)(l_3/l_1)$ , varied from 0.44 for *G. menardii* to 0.87 for *O. universa*. The rate of molecular evolution,  $f_0\alpha$ , is calculated as  $f_0\alpha = D/2\Gamma$  (following Eq. 5), where  $D$  (substitutions nucleotide<sup>-1</sup>) is the genetic divergence between two taxa that shared a common ancestor  $\Gamma$  time units ago, and  $f_0$  is the fraction of mutations that are selectively neutral (following Eq. 5). Our model predicts that the rate of molecular evolution declines with increasing body size as  $f_0\alpha \propto M_i^{-1/4}$  (following Eqs. 1-5), so  $D \propto (M_1^{-1/4} + M_2^{-1/4})$  if temperature and  $\Gamma$  are both held constant. Consequently, the smaller-bodied taxon makes a greater contribution to the genetic divergence,  $D$ , and hence to the



estimated rate of molecular evolution,  $f_0\alpha$ . To account for the greater contribution of the smaller-bodied taxon to the estimate of  $f_0\alpha$ , we

calculate the overall body size of each taxon pair using the “quarter-power” average of mass (15):  $\langle M \rangle_q = \left( (M_1^{-1/4} + M_2^{-1/4}) / 2 \right)^{-4}$ .

**Temperature.** We estimated the habitat temperature,  $T_i$ , of each morphospecies using the Brown Foraminifera Database (BFD) (16) in conjunction with contemporary ocean temperature data (17). The BFD is comprised of 1,265 samples, resolved to morphospecies, for large counts of foraminifera shells in contemporary sediments ( $\bar{x} \pm \text{s.d.}$ :  $432 \pm 236$  individuals per sample). Most BFD samples were collected from tropical sites with sea-surface temperatures  $>25^\circ\text{C}$ . In order to use these data to estimate  $T_i$ , we first subdivided the 1,265 BFD samples into six habitat temperature bins ( $0\text{--}5^\circ\text{C}$ ,  $5\text{--}10^\circ\text{C}$ , ...  $25\text{--}30^\circ\text{C}$ ) by using temperature data in the World Ocean Database (17). We then estimated

the habitat temperature of each taxon as  $T_i = \sum_{j=1}^{j=6} P_{i,j} \bar{T}_j / \sum_{j=1}^{j=6} P_{i,j}$ , where  $\bar{T}_j$  is the temperature midpoint of bin  $j$  ( $\bar{T}_1 = 2.5^\circ\text{C}$ ,  $\bar{T}_2 = 7.5^\circ\text{C}$ , ...  $\bar{T}_6$

$= 27.5^\circ\text{C}$ ), and  $P_{i,j}$  is the average proportional abundance of species  $i$  in bin  $j$  of the BFD samples. We used mean annual sea-surface temperature data (17) to bin the BFD samples and estimate habitat temperatures for shallow-water dwellers (S) and mean annual temperatures at 200-m depth (17) to bin the samples and estimate habitat temperatures for deeper-water dwellers (D). Two published sources were used to assign taxa to these categories (ref. 18 and <http://palaeo.gly.bris.ac.uk/Data/plankrange.html>). Our model predicts that the rate of molecular evolution increases exponentially with temperature according to the Boltzmann relationship (following Eqs. 1-5), so  $D \propto (e^{-E/kT_1} + e^{-E/kT_2})$  if

$\Gamma$  and body mass and are both held constant. Consequently, the taxon occurring in the warmer environment makes a greater contribution to

the genetic divergence,  $D$ , and hence to the estimated rate of molecular evolution,  $f_0\alpha$ . To control for the greater contribution of the warmer-bodied taxon to the estimate of  $f_0\alpha$ , we characterized the overall habitat temperature of each taxon pair by using the Boltzmann average:

$\langle T \rangle_E = -E / \ln((e^{-E/kT_1} + e^{-E/kT_2})/2)k$ , where  $T_1$  and  $T_2$  are both in Kelvins. Please note that we report  $T_1$ ,  $T_2$ , and  $\langle T \rangle_E$  in units of °C in the table above for clarity of presentation but that  $1/k\langle T \rangle_E$  is calculated based on absolute habitat temperature in units of Kelvin.

**Evolutionary Rates for SSU rDNA.** Estimates of overall genetic divergence,  $D$ , in the SSU rDNA gene, minimum and maximum divergence times,  $\Gamma_{\min}$  and  $\Gamma_{\max}$  (in Ma) were obtained from the sources cited in the table above. If  $D$  was reported in multiple sources, the arithmetic average of the different estimates was taken. The rate of molecular evolution ( $f_0\alpha$ , % substitutions•nucleotide<sup>-1</sup>•Ma<sup>-1</sup>) was then calculated as  $f_0\alpha = D / (\Gamma_{\min} + \Gamma_{\max})$ . It is important to recognize that our methods of estimating body size,  $\langle M \rangle_q$ , and temperature,  $\langle T \rangle_E$ , assume that extant taxa are similar in size to and occur in similar thermal environments as their common ancestors (15). We therefore excluded from analysis the only microperforate pair of planktonic foraminifera with genetic divergence data, *Globigerinita uvula* and *Globigerinita glutinata*, because molecular evidence indicates that both taxa diverged from a benthic lineage relatively recently (2) and may therefore differ considerably in size and/or habitat temperature from their common ancestor.

1. Kennett, J. P. & Srinivasan, S. (1983) *Neogene Planktonic Foraminifera: A Phylogenetic Atlas* (Hutchinson Ross, Stroudsburg, Pennsylvania).
2. Stewart, I. A., Darling, K. F., Kroon, D., Wade, C. M. & Troelstra, S. R. (2001) *Mar. Micropaleontol.* **43**, 143-153.
3. de Vargas, C., Zaninetti, L., Hilbrecht, H. & Pawlowski, J. (1997) *J. Mol. Evol.* **45**, 285-294.
4. de Vargas, C. & Pawlowski, J. (1998) *Mol. Phylogenet. Evol.* **9**, 463-469.
5. de Vargas, C., Bonzon, M., Rees, N. W., Pawlowski, J. & Zaninetti, L. (2002) *Mar. Micropaleontol.* **45**, 101-116.
6. Huber, B. T., Bijma, J. & Darling, K. (1997) *Paleobiology* **23**, 33-62.
7. Darling, K. F., Wade, C. M., Kroon, D. & Brown, A. J. L. (1997) *Mar. Micropaleontol.* **30**, 251-266.
8. Darling, K. F., Wade, C. M., Kroon, D., Brown, A. J. L. & Bijma, J. (1999) *Paleoceanography* **14**, 3-12.
9. Pawlowski, J., Bolivar, I., Fahrni, J. F., deVargas, C., Gouy, M. & Zaninetti, L. (1997) *Mol. Biol. Evol.* **14**, 498-505.
10. Darling, K. F., Kucera, M., Pudsey, C. J. & Wade, C. M. (2004) *Proc. Natl. Acad. Sci. USA* **101**, 7657-7662.
11. Darling, K. F., Kucera, M., Wade, C. M., von Langen, P. & Pak, D. (2003) *Paleoceanography* **18**.
12. de Vargas, C., Renaud, S., Hilbrecht, H. & Pawlowski, J. (2001) *Paleobiology* **27**, 104-125.
13. Norris, R. D. (1990) Ph.D. thesis (Harvard University, Boston), p. 294.
14. Be, A. W. H. (1977) in *Oceanic Micropaleontology*, ed. Ramsay, A. T. S. (Academic, London), Vol. 1, pp. 1-100.

15. Gillooly, J. F., Allen, A. P., West, G. B. & Brown, J. H. (2005) *Proc. Natl. Acad. Sci. USA* **102**, 140-145.
16. Prell, W., Martin, A., Cullen, J. & Trend, M. (1999) *The Brown University Foraminiferal Database* (National Oceanic & Atmospheric Administration<949>National Geophysical Data Center Paleoclimatology Program, Boulder, CO).
17. Conkright, M. E., Antonov, J. I., Baranova, O., Boyer, T. P., Garcia, H. E., Gelfeld, R., Johnson, D., Locarnini, R. A., Murphy, P. P., O'Brien, T. D., *et al.* (2002) *World Ocean Databas* (U.S.Government Printing Office, Washington, DC), Vol. 1.
18. Hilbrecht, H. (1996) in *Mitteilungen aus dem Geologischen Institut der Eidgen* (Technischen Hochschule und der Universität Zürich, Zurich), pp. 93.



## Appendix 2

Genetic divergences among cryptic genotypes,  $D_s$ , were compiled from the sources cited below. If  $D_s$  was reported in multiple sources, then the arithmetic average of the different estimates was taken. Habitat temperatures for each taxon pair,  $T_1$  and  $T_2$ , were estimated from the latitude/longitude coordinates where genotypes were sampled using mean annual sea-surface temperature data (1) for shallow-water morphospecies (S), and mean annual temperatures at 200-m depth (1) for deeper-water morphospecies (D). Two published sources were used to assign taxa to these categories (ref. 2 and <http://palaeo.gly.bris.ac.uk/Data/plankrange.html>). The overall habitat temperature of each taxon pair was then calculated using the Boltzmann average,  $\langle T \rangle_E = -E / \ln((e^{-E/kT_1} + e^{-E/kT_2})/2)k$ . Please note that  $T_1$ ,  $T_2$ , and  $\langle T \rangle_E$  are reported below in units of degrees Celsius for clarity, but that  $1/k\langle T \rangle_E$  is calculated based on absolute temperature in Kelvins. Habitat descriptions for each cryptic genotype listed below are summarized in ref. 3.

|                                  | Genotype 1                   | Genotype 2                    | Temperature (°C) |       |                       | Divergence |         |                          |            |
|----------------------------------|------------------------------|-------------------------------|------------------|-------|-----------------------|------------|---------|--------------------------|------------|
| Morphospecies                    | (Latitude / Longitude)       | (Latitude / Longitude)        | $T_1$            | $T_2$ | $\langle T \rangle_E$ | $D_s$      | Sources | $1/k\langle T \rangle_E$ | $\ln(D_s)$ |
| <i>Globigerina bulloides</i> (D) | Type Ia<br>(-14.5° / 145.5°) | Type Ib<br>(43.5° / 8.5°)     | 20               | 13    | 17                    | 0.051      | (4)     | 39.96                    | -2.98      |
| <i>Globigerina bulloides</i> (D) | Type IIa<br>(61.5° / -35.5°) | Type IIb<br>(59.5° / -22.5°)  | 5                | 9     | 7                     | 0.039      | (4, 5)  | 41.44                    | -3.25      |
| <i>Globigerina bulloides</i> (D) | Type IIa<br>(61.5° / -35.5°) | Type IIc<br>(-52.5° / -56.5°) | 5                | 5     | 5                     | 0.032      | (5)     | 41.73                    | -3.45      |

|  | Genotype 1                           | Genotype 2                              | Temperature (°C) |       |                       | Divergence |         |                          |            |
|--|--------------------------------------|---|------------------|-------|-----------------------|------------|---------|--------------------------|------------|
| Morphospecies                            | (Latitude / Longitude)               | (Latitude / Longitude)                  | $T_1$            | $T_2$ | $\langle T \rangle_E$ | $D_s$      | Sources | $1/k\langle T \rangle_E$ | $\ln(D_s)$ |
| <i>Globigerina bulloides</i> (D)         | Type IIa<br>(61.5° / -35.5°)         | Type IIId<br>(32.5° / -118.5°)          | 5                | 9     | 7                     | 0.043      | (4, 5)  | 41.44                    | -3.15      |
| <i>Globigerina bulloides</i> (D)         | Type IIb<br>(59.5° / -22.5°)         | Type IIc<br>(-52.5° / -56.5°)           | 9                | 5     | 7                     | 0.050      | (5)     | 41.45                    | -3.00      |
| <i>Globigerina bulloides</i> (D)         | Type IIb<br>(59.5° / -22.5°)         | Type IIId<br>(32.5° / -118.5°)          | 9                | 9     | 9                     | 0.018      | (4, 5)  | 41.20                    | -4.01      |
| <i>Globigerina bulloides</i> (D)         | Types Ia/Ib<br>(-14.5° / 145.5°)     | Types IIa/IIb/IIId<br>(-55.5° / -60.5°) | 20               | 4     | 15                    | 0.090      | (4, 6)  | 40.32                    | -2.41      |
| <i>Globigerinella siphonifera</i> (D)    | Type I<br>(12.5° / -68.5°)           | Type IIa<br>(12.5° / -68.5°)            | 17               | 17    | 17                    | 0.062      | (7, 8)  | 39.99                    | -2.78      |
| <i>Globigerinella siphonifera</i> (D)    | Type I<br>(12.5° / -68.5°)           | Types IIa/IIb<br>(12.5° / -68.5°)       | 17               | 17    | 17                    | 0.040      | (6)     | 39.99                    | -3.22      |
| <i>Globigerinella siphonifera</i> (D)    | Type IIa<br>(12.5° / -68.5°)         | Type IIb<br>(32.5° / -118.5°)           | 17               | 9     | 14                    | 0.011      | (6)     | 40.48                    | -4.51      |
| <i>Globigerinoides ruber</i> (S)         | pink<br>(12.5° / -68.5°)             | Type Ia<br>(-14.5° / 145.5°)            | 27               | 27    | 27                    | 0.056      | (7, 8)  | 38.66                    | -2.89      |
| <i>Globigerinoides ruber</i> (S)         | pink<br>(12.5° / -68.5°)             | Types Ia/Ib<br>(17.5° / -67.5°)         | 27               | 28    | 27                    | 0.055      | (6)     | 38.61                    | -2.90      |
| <i>Globigerinoides ruber</i> (S)         | pink/Types Ia/Ib<br>(12.5° / -68.5°) | Type II<br>(32.5° / -118.5°)            | 27               | 16    | 23                    | 0.108      | (6)     | 39.19                    | -2.23      |
| <i>Globorotalia truncatulinoides</i> (D) | Type 1<br>(-22.5° / -36.5°)          | Type 2<br>(-27.5° / -40.5°)             | 18               | 17    | 18                    | 0.036      | (9)     | 39.93                    | -3.34      |
| <i>Globorotalia truncatulinoides</i> (D) | Type 1<br>(-22.5° / -36.5°)          | Type 3<br>(-37.5° / -50.5°)             | 18               | 14    | 16                    | 0.064      | (9)     | 40.09                    | -2.76      |
| <i>Globorotalia truncatulinoides</i> (D) | Type 1<br>(-22.5° / -36.5°)          | Type 4<br>(-46.5° / -56.5°)             | 18               | 4     | 13                    | 0.059      | (9)     | 40.52                    | -2.83      |
| <i>Globorotalia truncatulinoides</i> (D) | Type 2                               | Type 3                                  | 17               | 14    | 15                    | 0.064      | (9)     | 40.22                    | -2.76      |

|  | Genotype 1                      | Genotype 2                        | Temperature (°C) |       |                       | Divergence |             |                          |            |
|--|---------------------------------|-----------------------------------|------------------|-------|-----------------------|------------|-------------|--------------------------|------------|
| Morphospecies                            | (Latitude / Longitude)          | (Latitude / Longitude)            | $T_1$            | $T_2$ | $\langle T \rangle_E$ | $D_s$      | Sources     | $1/k\langle T \rangle_E$ | $\ln(D_s)$ |
|  | (-27.5° / -40.5°)               | (-37.5° / -50.5°)                 |                  |       |                       |            |             |                          |            |
| <i>Globorotalia truncatulinoides</i> (D) | Type 2<br>(-27.5° / -40.5°)     | Type 4<br>(-46.5° / -56.5°)       | 17               | 4     | 12                    | 0.062      | (9)         | 40.69                    | -2.79      |
| <i>Globorotalia truncatulinoides</i> (D) | Type 3<br>(-37.5° / -50.5°)     | Type 4<br>(-46.5° / -56.5°)       | 14               | 4     | 10                    | 0.012      | (9)         | 40.97                    | -4.42      |
| <i>Neogloboquadrina pachyderma</i> (D)   | Type III<br>(-55.5° / -60.5°)   | Type IV<br>(-65.5° / -75.5°)      | 4                | 1     | 3                     | 0.124      | (5)         | 42.10                    | -2.09      |
| <i>Orbulina universa</i> (S)             | Caribbean<br>(12.5° / -68.5°)   | Mediterranean<br>(43.5° / 8.5°)   | 27               | 18    | 23                    | 0.104      | (6, 10, 11) | 39.14                    | -2.26      |
| <i>Orbulina universa</i> (S)             | Caribbean<br>(12.5° / -68.5°)   | Sargasso<br>(32.5° / -64.5°)      | 27               | 23    | 25                    | 0.173      | (11)        | 38.88                    | -1.75      |
| <i>Orbulina universa</i> (S)             | Mediterranean<br>(43.5° / 8.5°) | Sargasso<br>(32.5° / -64.5°)      | 18               | 23    | 21                    | 0.120      | (11)        | 39.52                    | -2.12      |
| <i>Turborotalita quinqueloba</i> (S)     | Type I<br>(-14.5° / 145.5°)     | Types IIa/IIb<br>(59.5° / -22.5°) | 27               | 10    | 21                    | 0.058      | (4)         | 39.46                    | -2.85      |
| <i>Turborotalita quinqueloba</i> (S)     | Type IIa<br>(59.5° / -22.5°)    | Type IIb<br>(59.5° / -22.5°)      | 10               | 10    | 10                    | 0.077      | (4, 5)      | 41.02                    | -2.57      |
| <i>Turborotalita quinqueloba</i> (S)     | Type IIa<br>(59.5° / -22.5°)    | Type IIc<br>(32.5° / -118.5°)     | 10               | 16    | 14                    | 0.070      | (5)         | 40.49                    | -2.66      |
| <i>Turborotalita quinqueloba</i> (S)     | Type IIb<br>(59.5° / -22.5°)    | Type IIc<br>(32.5° / -118.5°)     | 10               | 16    | 14                    | 0.007      | (5)         | 40.49                    | -4.98      |

1. Conkright, M. E., Antonov, J. I., Baranova, O., Boyer, T. P., Garcia, H. E., Gelfeld, R., Johnson, D., Locarnini, R. A., Murphy, P.

P., O'Brien, T. D., *et al.* (2002) *World Ocean Database*(U.S.Government Printing Office, Washington, DC), Vol.1.

2. Hilbrecht, H. (1996) in *Mitteilungen aus dem Geologischen Institut der Eidgen (Technischen Hochschule und der Universität Zürich, Zurich, Switzerland)*, pp. 93.
3. Kucera, M. & Darling, K. F. (2002) *Philos. Trans. R. Soc. London A* **360**, 695-718.
4. Stewart, I. A., Darling, K. F., Kroon, D., Wade, C. M. & Troelstra, S. R. (2001) *Mar. Micropaleontol.* **43**, 143-153.
5. Darling, K. F., Wade, C. M., Stewart, I. A., Kroon, D., Dingle, R. & Brown, A. J. L. (2000) *Nature* **405**, 43.
6. Darling, K. F., Wade, C. M., Kroon, D., Brown, A. J. L. & Bijma, J. (1999) *Paleoceanography* **14**, 3-12.
7. Darling, K. F., Wade, C. M., Kroon, D. & Brown, A. J. L. (1997) *Mar. Micropaleontol.* **30**, 251-266.
8. Huber, B. T., Bijma, J. & Darling, K. (1997) *Paleobiology* **23**, 33-62.
9. de Vargas, C., Renaud, S., Hilbrecht, H. & Pawlowski, J. (2001) *Paleobiology* **27**, 104-125.
10. de Vargas, C., Zaninetti, L., Hilbrecht, H. & Pawlowski, J. (1997) *J. Mol. Evol.* **45**, 285-294.
11. de Vargas, C., Norris, R., Zaninetti, L., Gibb, S. W. & Pawlowski, J. (1999) *Proc. Natl. Acad. Sci. USA* **96**, 2864-2868.



### Appendix 3

The latitudinal distribution of foraminifera first occurrences (FOs) was analyzed by using the Neptune database (1), which is comprised of >50,000 records of foraminifera occurrence in >3,000 samples collected from deep-sea drilling cores around the world. The Neptune database has been made publicly available thanks to two major initiatives, Chronos (<http://www.chronos.org>) and the Paleobiology Database (<http://paleodb.org>). For this study, we analyzed morphospecies-level data marked as valid based on the “resolved” taxonomy in the February 2006 version of Neptune downloaded from <http://paleodb.org>. Samples in Neptune were aged using biostratigraphy methods (1). To control for issues associated with this method of age estimation, samples within 0.36 Ma years of hiatuses (periods of negligible sediment accumulation) were excluded based on a published delineation of hiatuses (2) and the reported precision of Neptune age estimates, i.e.,  $\pm 0.36$  Ma for biostratigraphy events in the Paleogene (3). Data from the following drilling cores were excluded because inspection of published biostratigraphy plots (1) indicated that age estimates were too imprecise for our purposes: 62A, 64, 356, 369A, 433A, 470A, 588C, 700B, and 738B.

Our method of analysis explicitly controls for variation in the intensity of sampling effort and area, because these variables can significantly influence paleontological relationships (4, 5). To control for these variables, foraminifera samples were first assigned to one of four equal area bands of  $\sim 9.1 \times 10^7$  km<sup>2</sup> surface water each (90.00°S–36.11°S, 36.11°S–8.24°S, 8.24°S–18.87°N, 18.87°N–90.00°N), and one of six 5-Ma time intervals (0–5 Ma, ... , 25–30 Ma) by using sample age and paleolatitude

estimates in Neptune. Samples >30-Ma old were excluded from analysis, because the number of samples in Neptune declines precipitously beyond this date (1). A total of 3,728 foraminifera samples were included in our analysis, but sampling varied by more than an order of magnitude among latitudinal bands and time intervals, as shown in the table below.

|                 | 0-5 Ma | 5-10 Ma | 10-15 Ma | 15-20 Ma | 20-25 Ma | 25-30 Ma |
|-----------------|--------|---------|----------|----------|----------|----------|
| 90.00°S–36.11°S | 123    | 42      | 109      | 98       | 58       | 110      |
| 36.11°S–8.24°S  | 363    | 175     | 93       | 51       | 47       | 116      |
| 8.24°S–18.87°N  | 437    | 316     | 139      | 40       | 74       | 70       |
| 18.87°N–90.00°N | 947    | 105     | 92       | 18       | 56       | 49       |

To control for this substantial variation in sampling effort, 40 samples were selected at random and without replacement from each of the four latitudinal bands and six time intervals. The total number of samples in this subset of data was slightly less than 960 ( $= 40 \times 4 \times 6$ ) because one latitudinal-band/time-interval combination (18.87°N–90.00°N/15–20 Ma) had only 18 samples (see table above). The average speciation rate in each latitudinal band over the 30-Ma time interval was estimated from the 942-sample subset by determining the latitudinal band of FO for each newly observed foraminifera morphospecies and then tallying the total number of FOs for each band. To prevent taxa that may have arisen >30 Ma ago from entering into our calculations, we excluded morphospecies with FO estimates >27.5-Ma old in the full 3,728-sample dataset. A total of 100 942-sample subsets were generated by using the randomization procedure described above to generate the 95% confidence intervals (CIs) depicted in Fig. 3B for the FO rates.

1. Spencer-Cervato, C. (1999) *Palaeontologia Electronica* **2** (2), article 4.
2. Spencer-Cervato, C. (1998) *Paleoceanography* **13**, 178-182.
3. Spencer-Cervato, C., Thierstein, H. R., Lazarus, D. B. & Beckmann, J. P. (1994)  
*Paleoceanography* **9**, 739-763.
4. Alroy, J., Marshall, C. R., Bambach, R. K., Bezusko, K., Foote, M., Fursich, F. T.,  
Hansen, T. A., Holland, S. M., Ivany, L. C., Jablonski, D., *et al.* (2001) *Proc.*  
*Natl. Acad. Sci.* **98**, 6261-6266.
5. Barnosky, A. D., Carrasco, M. A. & Davis, E. B. (2005) *PLoS Biology* **3**, e266.

## Appendix 4

Paleontological evidence indicates that equatorial sea-surface temperatures have remained similar to those of today for the past 30 Ma (1) but that ocean temperatures at the poles have cooled  $\approx 8^\circ\text{C}$  over this time period from a peak of  $\approx 4^\circ\text{C}$  at the Oligocene-Miocene transition to about  $-4^\circ\text{C}$  today (2). Our analysis explicitly accounts for these spatial and temporal trends in sea-surface temperatures. Given the uncertainties associated with paleotemperature estimates, it is reasonable to assume that equatorial sea-surface temperatures,  $T_0$ , have remained constant at  $\approx 301\text{ K}$  ( $= 28^\circ\text{C}$ ) over the past 30 Ma (1, 2). Furthermore, because deep ocean waters are derived primarily from the cooling and sinking of surface waters, it is also reasonable to assume that deep-sea paleotemperatures serve as a proxy for high-latitude sea-surface paleotemperatures at both the North and South Poles (2). Consequently, changes in sea-surface temperature with latitude,  $L$ , should be approximately symmetric about the equator. We modeled changes in sea-surface temperature (in Kelvins) with latitude,  $L$  ( $-90^\circ$  to  $90^\circ\text{N}$ ), and time,  $t$  ( $-30\text{ Ma}$  to  $0$ ), by using the heat equation on the surface of a sphere:

$$T(L, t) = (P(t) - T_0) \sin^2(\pi L / 180) + T_0 \quad (\text{A1})$$

where  $L = -90^\circ\text{N}$  corresponds to the South Pole,  $T_0$  is the sea-surface temperature at the equator (i.e.,  $L = 0^\circ\text{N}$ ), which was assumed to remain constant at  $301\text{ K}$  over the 30-Ma time interval, and  $P(t)$  is sea-surface temperature at the poles (in Kelvins) at time  $t$ .

Here  $P(t)$  was taken to be the robust deep-sea paleotemperature calibration in Fig. 2 of ref. 2. The heat equation (Eq. **A1**) does an excellent job of characterizing latitudinal trends in contemporary sea-surface temperatures (3), as shown by the close



correspondence between the empirical data, represented by closely overlapping circles defining a thickened line in the figure below, and the thinner, fitted line ( $r^2 = 0.98$ ;  $T_0 = 301.4 \text{ K} = 28.4^\circ\text{C}$ ,  $P(0) = 268.8 \text{ K} = -4.2^\circ\text{C}$ ). Eq. **A1** was fitted to the contemporary data using nonlinear least-squares regression.

Using Eq. **A1**, we estimated the area-weighted average of  $1/kT$  in each latitudinal band over the past 30 Ma as

$$\overline{1/kT} = \left( \frac{1}{30} \right) \int_{t=-30}^{t=0} \left( \frac{1}{9.1 \times 10^7} \right) \int_{L=L_1}^{L=L_2} A(L)(1/kT(L,t))dLdt \quad (\text{A2})$$

where  $A(L)dL$  is ocean

area ( $\text{km}^2$ ) in the

incremental latitudinal

band centered on  $L$  ( $-90^\circ$

to  $90^\circ\text{N}$ ) of width  $dL$ , and

$L_1$  and  $L_2$  are the limits of

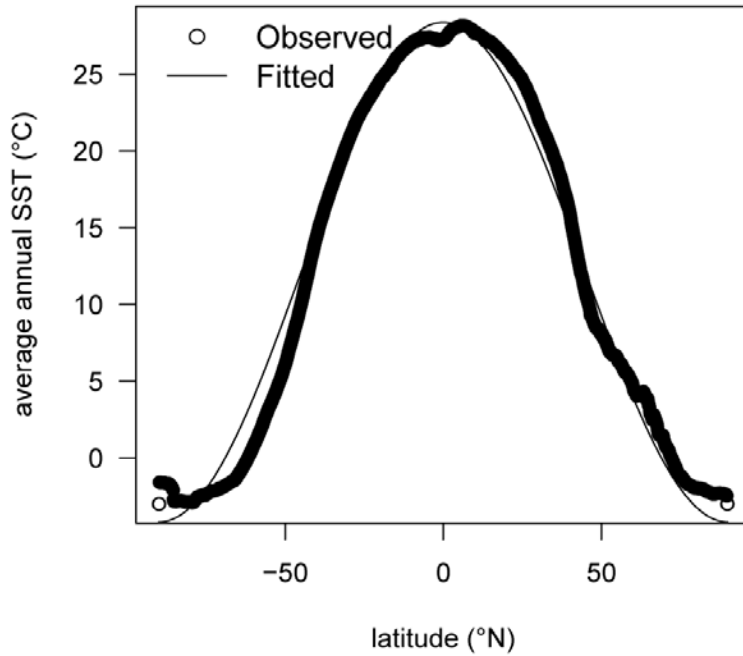
integration for each of the

four  $\approx 9.1 \times 10^7 \text{ km}^2$

latitudinal bands ( $-90^\circ\text{N}$

to  $-36.11^\circ\text{N}$ ,  $-36.11^\circ\text{N}$  to

$-8.24^\circ\text{N}$ ,  $-8.24^\circ\text{N}$  to  $18.87^\circ\text{N}$ ,  $18.87^\circ\text{N}$  to  $90^\circ\text{N}$ ).



1. Crowley, T. J. & Zachos, J. C. (2000) in *Warm Climates in Earth History* (Cambridge Univ. Press, New York), pp. 50-76.

2. Zachos, J., Pagani, M., Sloan, L., Thomas, E. & Billups, K. (2001) *Science* **292**, 686-693.
3. Casey, K. S. & Cornillon, P. (1999) *J. Climate* **12**, 1848-1863.

## Appendix 5

**Estimating the Temperature Dependence of Community Abundance.** Our model yields predictions on the temperature dependence of per capita speciation rate (Eq. 8). Evaluating this prediction required that we explicitly account for temperature-dependent changes in foraminifera abundance across latitudes. In order to avoid difficulties associated with inferring live abundances of foraminifera from accumulation rates of foraminifera tests in sediments (1), we characterized the temperature dependence of foraminifera abundance by using data compiled in the 2001 World Ocean Database (WOD) (2). This approach assumes that foraminifera communities are strongly and directly regulated by temperature, an assumption that is supported by the successful use of community data from fossilized foraminifera for paleotemperature reconstruction (for an example, see ref. 3). The WOD contains samples collected in oceans throughout the world over a time period spanning >50 years. Planktonic foraminifera occur near the ocean surface to depths that exceed 200 m (4). We therefore characterized the temperature dependence of abundance by using all WOD volumetric estimates (individuals  $\text{m}^{-3}$ ) for foraminifera (WOD Biological Group code 303000; Integrated Taxonomic Information System code 44030) that were obtained with net tows that extended from the ocean surface (= 0 m) to depths at or below the thermocline (maximum depth cutoff  $\leq 250$  m). Abundance estimates meeting these criteria ( $n = 1,744$ ) were regressed against mean annual sea surface temperature data (5) by using an ordinary least-squares (OLS) model,  $\ln(J_A) = E_J(1/kT) + \ln(j_o)$ , to estimate parameters of the following function:

$$J_A(T) = j_o e^{E_J/kT} \quad (\text{A3})$$

where  $J_A(T)$  is total foraminifera abundance per unit area over the depth range 0–250 m (individuals  $\text{km}^{-2}$ ),  $T$  is mean annual sea surface temperature in Kelvins,  $E_J$  (eV)

characterizes the

temperature dependence

of abundance ( $E_J = 0.45$

eV; OLS-estimated

95% CI, 0.37–0.52 eV),

and  $j_o$  is a normalization

constant (OLS estimate

of 20 individuals  $\text{km}^{-2}$ ).

The variance explained

by the model is low

(OLS  $r^2 = 0.08$ ), consistent with empirical observations that seasonal fluctuations in

foraminifera abundance at a site generally exceed an order of magnitude (6, 7).

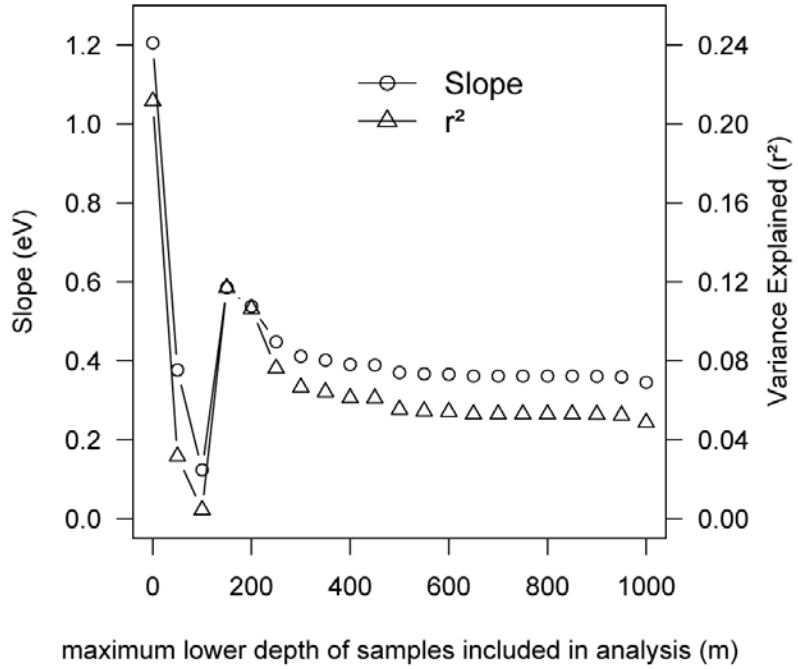
Nevertheless, the model is highly significant ( $P < 10^{-15}$ ). Furthermore, regardless of the

maximum lower depth cutoff used to screen samples (0–1,000 m), the slope  $E_J$  is always

positive, indicating pronounced declines in foraminifera abundance in relation to

increasing sea surface temperature. Finally, for all lower depth cutoffs  $>250$  m, the slope

and  $r^2$  value of the fitted model show little change, as shown in the figure above.



**Estimating the Temperature Dependence of the per Capita Speciation Rate.** Using

$J_A(T)$  (Eq. A3) and  $T(L, t)$  (Eq. A1 in Appendix 4), we can evaluate the predicted

temperature dependence of per capita speciation rate while explicitly controlling for latitudinal changes in foraminifera abundance and ocean temperatures over the past 30 Ma. Combining Eqs. **A1-A3** with Eq. **9** yields an expression for the cumulative latitudinal distribution of foraminifera FOs over the time interval  $t = -30$  Ma to  $t = 0$ :

$$F(L) = \int_{t=-30}^{t=0} \int_{L'=-90}^{L'=L} f(L',t) dL' dt \bigg/ FO_{Tot} = \int_{t=-30}^{t=0} \int_{L'=-90}^{L'=L} A(L') e^{(E_J - E)/kT(L',t)} dL' dt \bigg/ FO_{Tot} \quad (\text{A4})$$

where  $F(L)$  is the fraction of all FOs observed globally ( $FO_{Tot}$ ) over the past 30 Ma that occur between the latitudes  $-90^\circ\text{N}$  and  $L$ , and  $f(L,t)dL = A(L)j_o\nu_oB_o e^{(E_J - E)/kT(L,t)} dL$  is the theoretically predicted FO rate in the latitudinal band center on  $L$  of width  $dL$  and ocean area  $A(L)dL$  at time  $t$  ( $\text{FO sec}^{-1}$ ) (following Eqs. **8** and **9**). Eq. **A4** has just one fitted parameter,  $E - E_J$ , which we estimated for each of the 100 sets of standardized FO data generated by randomization as described in Appendix 3. We fit the predicted distribution (Eq. **A4**) to the empirical data by finding the value of  $E_J - E$  that minimized Kuiper's statistic (8). Like the Kolmogorov–Smirnov (K–S) statistic, Kuiper's statistic characterizes the difference between two cumulative distributions. For our analysis, Kuiper's statistic is preferable to K–S because it is equally sensitive to differences between observed and predicts cumulative distributions at all values of  $L$ . By fitting each of the 100 sets of standardized FO data to Eq. **A4**, we generated the 95% CI for  $E - E_J$  (0.25–0.44 eV). These CIs were added to those for  $E_J$  (OLS-estimated 95% CI; 0.37–0.52 eV) to obtain the 95% CI for  $E$  (95% CI; 0.62–0.96 eV).

### **Estimating the Normalization Parameter $\nu_o$ for the per Capita Speciation Rate.**

Combining Eqs. **A2**, **A3**, and **9** yields

$$v_o = (V_m / A_m j_o) e^{(E-E_j)(\overline{1/kT})} \quad (\text{A5})$$

For the equal-area latitudinal bands 1-4 depicted in Fig. 2A, the respective estimates for  $V_m$  are 0.70, 1.68, 1.90, and 0.83 FO Ma<sup>-1</sup>, and the respective estimates for  $\overline{1/kT}$  are 40.66, 39.01, 38.58, and 40.07 eV<sup>-1</sup>. Taking  $j_o$  to be 20 individuals km<sup>-2</sup>,  $E$  to be 0.65 eV,  $Ej$  to be 0.45 eV, and  $A_m$  to be  $9.1 \times 10^7$  km<sup>2</sup> in Eq. **A5**, we obtain an estimate of  $v_o \approx 5.6 \times 10^{-20}$  species•individual<sup>-1</sup>•sec<sup>-1</sup>.

1. Murray, J. W. (1991) *Ecology and Paleoecology of Benthic Foraminifera* (Wiley, New York).
2. Conkright, M. E., Antonov, J. I., Baranova, O., Boyer, T. P., Garcia, H. E., Gelfeld, R., Johnson, D., Locarnini, R. A., Murphy, P. P., O'Brien, T. D., *et al.* (2002) *World Ocean Database* (U.S.Government Printing Office, Washington, DC), Vol.1.
3. Nikolaev, S. D., Oskina, N. S., Blyum, N. S. & Bubenshchikova, N. V. (1998) *Global Planet. Change* **18**, 85-111.
4. Fairbanks, R. G., Wiersma, P. H. & Beck, A. W. H. (1980) *Science* **207**, 61-63.
5. Casey, K. S. & Cornillon, P. (1999) *J. Climate* **12**, 1848-1863.
6. Bijma, J., Erez, J. & Hemleben, C. (1990) *J. Foramin. Res.* **20**, 117-127.
7. Thunell, R. C., Curry, W. B. & Honjo, S. (1983) *Earth Planet. Sci. Lett.* **64**, 44-55.
8. Press, W. H., Teukolsky, S. A., Vetterling, W. T. & Flannery, B. P. (1992) *Numerical Recipes in C* (Cambridge Univ. Press, New York).